

# POLYMER NANOCOMPOSITES BASED ON REACTIVE BLENDS OF PETG-BLOCK-PTMO CONTAINING HYBRID SYSTEM OF NANOFILLERS

Sandra Paszkiewicz<sup>1</sup>, Elzbieta Piesowicz<sup>1</sup>, Izabela Irska<sup>1</sup>, Daria Pawlikowska<sup>1</sup>, Anna Szymczyk<sup>2</sup> and Zbigniew Roslaniec<sup>1</sup>

<sup>1</sup> West Pomeranian University of Technology, Institute of Materials Science and Engineering, al. Piastow 19, PL70310 Szczecin, Poland, spaszkwicz@zut.edu.pl, www.zut.edu.pl

<sup>2</sup> West Pomeranian University of Technology, Institute of Physics, al. Piastow 48, PL70311 Szczecin, Poland,

**Keywords:** Reactive blends, Hybrid nanofillers, Polymer nanocomposites, Morphology, Electrical conductivity

## ABSTRACT

Single-Walled Carbon Nanotubes/ Graphene Nanoplatelets/ Carbon Black/PETG-*block*-PTMO hybrid nanocomposites were synthesized via in situ polymerization, that consisted of glycolysis of PETG post-consumer foil and subsequently polycondensation in the presence of poly(tetramethylene oxide) (PTMO). A remarkable synergistic effect between GNPs, Carbon Black and SWCNTs on improving electrical and mechanical properties of nanocomposites based on block copolymers was observed. Partially miscible structure of the PETG-*block*-PTMO allowed for a uniform distribution of every single type of nanoparticles (1D- SWCNT, 2D-GNP and 3D- CB) and stabilized the structure in question. This enabled to observe a so-called “synergistic effect”, caused by the use of mixture of nanofillers that differ in shape, on enhancement of electrical, thermal and mechanical properties of the “modified” post-consumer material. SEM images of the PETG-*block*-PTMO nanocomposites displayed that hybrid nanofillers exhibited better distribution and compatibility than SWCNTs, GNPs and CB did individually. The observed “positive hybrid effect” in the case of modified post-consumer material (PETG) will allow to lower the final price of the finished product (suitable selection of properties at the optimum price), which can be characterized by novel functional properties.

## 1 INTRODUCTION

Nowadays, the field of polymer nanocomposite research is currently one of the most rapidly developing domains of cognitive work and applied engineering. Up to now, nanocomposites containing carbon nanotubes have sparked great attention among scientists and innovative research groups [1]. Same has been with other allotropic forms of carbon like graphene or carbon black. One can find graphene as a one atom thick, two-dimensional (2-D) sheet composed of sp<sup>2</sup> carbon atoms arranged in a honeycomb lattice [2] with a carbon-carbon bond length of 0.142 nm [3, 4]. It has proven to have a variety of exceptional intrinsic characteristics among which high electron mobility at room temperature (250 000 cm<sup>2</sup>/Vs) [5, 6], (where, unlike in the case of CNTs, chirality does not impede it's electrical conductivity), exceptional thermal conductivity (5000 W/mK) [7], and superior mechanical properties with Young's modulus of ~1 TPa and ultimate strength of 130 GPa [6] can be distinguished. Above mentioned characteristics, along with an extremely high surface area (theoretical limit: 2630 m<sup>2</sup>/g) and gas permeability [8], demonstrate graphene's unique potential for improving electrical, mechanical, thermal and gas barrier properties of polymers [9, 10]. Carbon black (3-D) is virtually pure elemental carbon in the form of colloidal particles that are produced by incomplete combustion or thermal decomposition of gaseous or liquid hydrocarbons under controlled conditions [11]. Carbon black is also in the top 50 industrial chemicals manufactured worldwide, based on annual (2016) tonnage. Carbon black is chemically and physically distinct from soot and black carbon, with most types containing greater than 97% elemental carbon arranged as aciniform (grape-like cluster)

particulate. On the contrary, typically less than 60% of the total particle mass of soot or black carbon is composed of carbon, depending on the source and characteristics of the particles (shape, size, and heterogeneity). Taking all above into consideration, a simultaneous introduction of three types of carbon nanofillers such as CNTs (a fibrous /linear filler - 1D), graphene (a plate filler - 2D) and CB (a powder and may seem desirable from the standpoint of their influence on electrical and mechanical qualities).

A proper dispersion of all types of nanofillers throughout a polymer matrix may result in obtaining specified physical characteristics, most important being the enhancement of mechanical properties and obtaining electrically conductive materials. All at a very low total concentration of nanofillers. Latest literature on the subject indicates that it was not yet possible to fully utilize the potential of applying a mixture of nanofillers that differ in shape, like carbon nanotubes, graphene nanoplatelets and carbon black in order to observe a so-called “synergistic effect” which in theory should result in a significant enhancement of properties of obtained materials. Indeed, a remarkable synergistic effect between multi-graphene platelets (MGPs) and multi walled carbon nanotubes (MWCNTs) causing an improvement of mechanical properties and thermal conductivity in epoxy composites has been studied [12]. However, obtaining similar results for thermoplastic polymer composites remains an unresolved and thus a noteworthy subject, hence it is widely undertaken by many research groups. Therefore, an addition of carbon nanoparticles to reactive polymer blends seems to be of great interest, since polymer blending is the most economic and versatile way of producing materials combining the desired properties of different polymers that will allow a wider usage of these materials.

This work is a part of a wider project with an objective to fabricate modified polymer materials based on post-consumer PETG foils. Therefore, in this study, PETG-*block*-PTMO based nanocomposites with hybrid fillers comprising of SWCNTs, GNPs and CB were developed in order to enhance mechanical characteristics along with obtaining electrical conductivity in these systems.

## 2. MATERIALS AND METHODS

### 2.1 Materials

For the glycol modified poly(ethylene terephthalate) (PETG)-*block*-PTMO synthesis were used following materials: granulated and vacuum dried (24h/60°C) post-consumer PETG foils; poly(tetramethylene oxide) glycol with molecular mass of 1000 g/mol (PTMG, Terathane 1000, DuPont, USA) were used as received; 1,2-ethanediol (ED) (Sigma - Aldrich), catalysts: zinc acetate (ester exchange catalyst)  $Zn(CH_3COO)_2$  (Sigma - Aldrich); antimony trioxide – polycondensation catalyst -  $Sb_2O_3$  (Sigma – Aldrich); thermal stabilizer Irganox 1010 (Ciba – Geigy, Switzerland).

### 2.2 Nanofillers

The following three types of nanofillers that differ in shape were used in this study:

- **As 1D-type nanofiller** - the single walled carbon nanotubes KNT 95 purchased from Grafen Chemical Industries (Grafen Co., located in Ankara, TURKEY). According to manufacturers' data: diameter: < 2 nm, EC: > 100 S/cm, length: 5 – 30  $\mu$ m, purity: >95 %, surface area: 380  $m^2/g$ .
- **As 2D-type nanofiller** – graphene nanoplatelets (GNP-ANG), purchased from ANGSTRON Materials (Dayton, Ohio, USA) in the form of a powder with the thickness of less than three graphene layers, average platelets size of up to 10  $\mu$ m, carbon content of ~97.0 % and the oxygen content of ~2.10 %.

- **As 3D-type nanofiller** – carbon black nanopowder (nCB) purchased from US Research Nanomaterials, Inc. (Houston, USA) with the purity of >95%, APS of 150nm content of H<sub>2</sub>O: <5%, content of ash: <3.2%, pH: 9.80 true Density: 0.38g/ml and electrical resistivity: 0.30 Ω.cm.

### 2.3 Synthesis of PETG-block-PTMO nanocomposites

The glycol modified poly(ethylene terephthalate) - block - poly(tetramethylene oxide) (PETG-*block*-PTMO) copolymer based nanocomposites with carbon nanotubes, graphene nanoplatelets and carbon black were prepared by *in situ* polymerization that constitutes of two main steps: glycolysis of PETG post-consumer foil and subsequently polycondensation in the presence of PTMO. The PETG-*block*-PTMO copolymer with the content of 50 wt % of PETG segments and 50 wt % of PTMO soft segments was used as nanocomposite polymer matrix. The process of *in situ* polymerization was preceded by a stage of nanofillers dispersion. For that purpose a specified amount of nanofillers (or the mixture of nanofillers) was mixed in a liquid substrate (1,2-ethanediol) during a 30 min period, alternately using a high speed stirrer and vibrations of an ultrasound stirrer. A ready dispersion was then put into a polycondensation reactor (Autoclave Engineers, Pennsylvania, USA) along with a first portion of catalyst. First stage of the reaction, the glycolysis process, was performed in the temperature of 250°C and under pressure of 5bar. After ca. 1h of glycolysis process, the second stage of synthesis, being the polycondensation process, was commenced. For this purpose PTMO mixed with thermal stabilizer (Irganox 1010), along with the second portion of catalyst were inserted. The temperature of the reaction was left at the level of 250 °C. However, unlike the first stage which was performed under nitrogen pressure, the polycondensation stage was carried out under reduced pressure (~20 Pa). In this case, the course of the reaction was monitored by observing the stirrer's torque. When the polymer/nanocomposite melt reached a high molecular mass, it was then extruded in the form of a thin wire. It was subsequently granulated and subjected to injection moulding procedure. The schematic illustration of the synthesis process is presented in Figure 1.

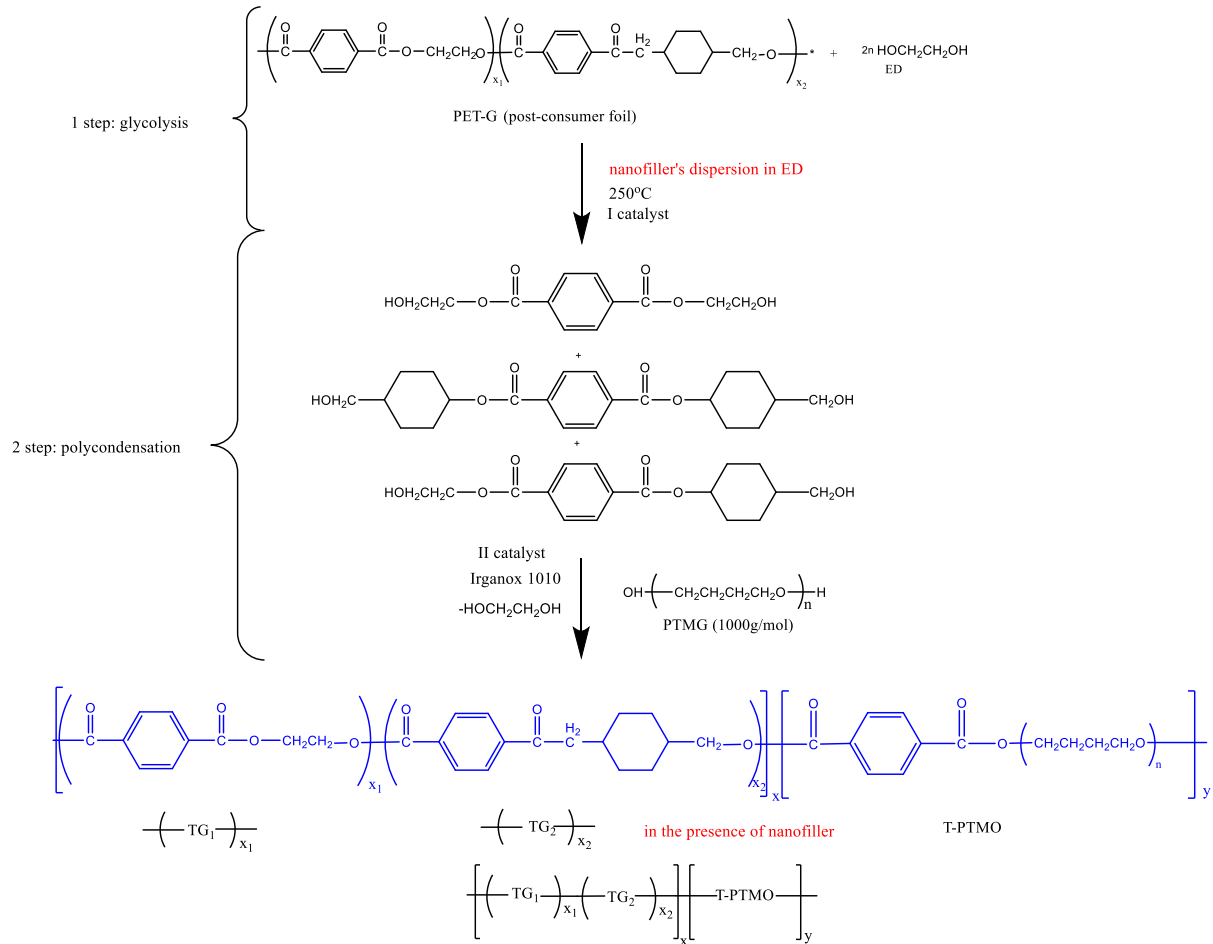


Figure 1: Scheme of the preparation process of PETG-*block*-PTMO based nanocomposites

## 2.4 Methods of characterization

The PETG and PETG-*block*-PTMO copolymers were compared by using an FTIR spectrophotometer (Bruker Optik GmbH model Tensor 27). Measurements were carried out using the attenuated total reflectance (ATR) technique. Each sample was scanned 32 times at the resolution of  $2 \text{ cm}^{-1}$  over the frequency range of  $4000\text{-}400 \text{ cm}^{-1}$ .

The structure nanocomposites were observed by scanning electron microscopy (SEM, JEOL JSM 6100 SEM). The samples were cryofractured in liquid nitrogen and then vacuum coated with a thin gold film before being analyzed using SEM.

The average number molecular mass was determined by using size exclusion chromatography (SEC) on a Waters GPC instrument, equipped with a Shimadzu LC-10AD pump, a WATERS 2414 differential refractive index detector (at  $35 \text{ }^\circ\text{C}$ ) and a MIDAS auto-injector (50mL injection volume) following the same procedure as described previously in [13].

The intrinsic viscosity  $[\eta]$  of the series of nanocomposites was determined at  $30 \text{ }^\circ\text{C}$  in the mixture of phenol/1,1,2,2-tetrachloroethane (60/40 by weight). The concentration of the polymer solution was of  $0.5 \text{ g/dl}$ . The measurement was carried using a capillary Ubbelohde viscometer (type Ic,  $K = 0.03294$ ).

The density of the dumbbell shape samples was measured at  $23 \text{ }^\circ\text{C}$  on hydrostatic scales (Radwag WPE 600C, Poland), calibrated according to standards with known density.

Melt flow index (MFI) was measured by using a melt indexer (CEAST, Italy) as weight of melt flow in grams per 10 min, at temperature of 195 °C, and at orifice diameter 2.095 mm and under 21.18 N load, according to ISO 1133 specification.

The amorphous structure of the samples was confirmed by differential scanning calorimeter (DSC). Measurements were carried out with a DSC1 (Mettler Toledo) which was calibrated for the temperature and melting enthalpy by using indium and n-octane as standards under a N<sub>2</sub> atmosphere with a heating rate of 10 K/min in the temperature range of 25 – 300 °C. Then, from the second heating the glass transition  $T_g$  and corresponding heat capacity were determined.

The electrical characterization of nanocomposites was conducted by means of a Novocontrol broadband dielectric spectrometer in the frequency range from 10<sup>-2</sup> Hz to 10<sup>7</sup> Hz, at room temperature. Therefore, circular gold electrodes (2 cm in diameter) were deposited onto the surfaces of the film samples by the sputtering technique. The complex dielectric permittivity  $\epsilon^* = \epsilon' - i\epsilon''$ , where  $\epsilon'$  represents the permittivity and  $\epsilon''$  the dielectric loss, was measured as a function of frequency (F) of the applied electric field. Electrical conductivity was calculated from equation:  $\sigma(F) = \epsilon_0 2\pi F \epsilon''$ , where  $\epsilon_0$  is the vacuum permittivity [14].

The tensile properties of the prepared PETG-block-PTMO based nanocomposites were measured using Autograph AG-X plus (Shimadzu) tensile testing machine equipped with a 1 kN Shimadzu load cell, an contact optical long travel extensometer and the TRAPEZIUM X computer software, operated at a constant crosshead speed of 100 mm/min. Measurements were performed at room temperature on the dumbbell samples with the grip distance of 20mm. According to DIN 53455 standard, the tensile modulus, stress at 100% strain, yield stress and strain, stress and elongation at break of the block copolymers were determined. Five measurements were conducted for each sample, and the results were averaged to obtain a mean value.

### 3 RESULTS AND DISCUSSION

Figure 2 shows the FTIR spectra of the prepared PETG foil and PETG-block-PTMO copolymer, in which the peak at 1712 cm<sup>-1</sup> displays the C=O of ester groups, and the C-H out-of-plane deformation of two carbonyl substituents on the aromatic ring depicts at 730 cm<sup>-1</sup> [15, 16]. The two peaks at 1410 and 1240 cm<sup>-1</sup> are ascribed to -CH<sub>2</sub>- deformation band and C(O)-O stretching of ester groups, respectively [16]. However, in PETG-block-PTMO copolymer, the peaks attributed to C-H stretching were shifted to the lower wavenumbers at 2852 and 2924 cm<sup>-1</sup> which is due to the presence of methyl groups in the structure of this polymer [17, 18]. Moreover, the C-H stretching peak of cyclohexylene ring was found at 958 cm<sup>-1</sup>.

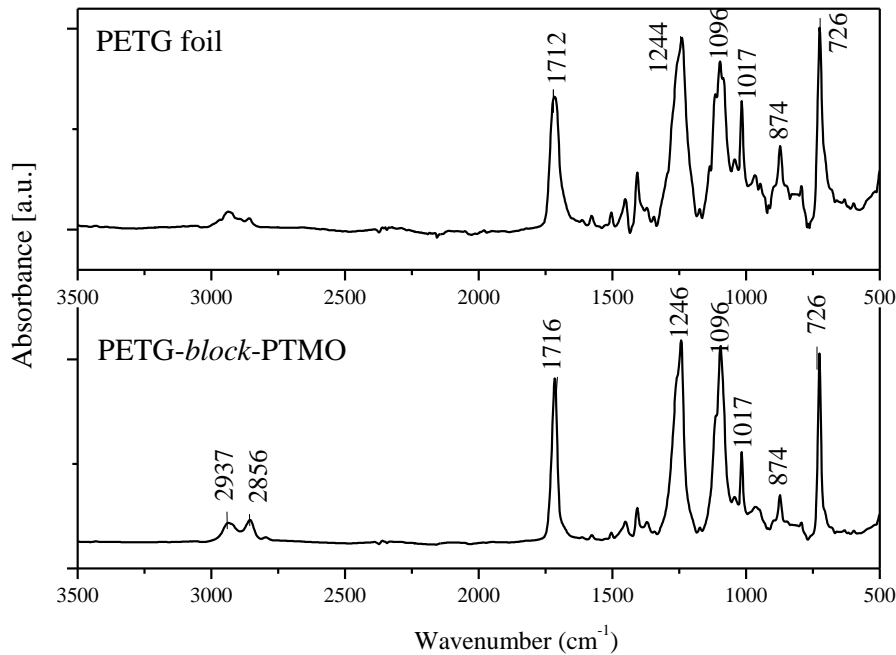


Figure 2: . FTIR spectrum of PETG foil and PETG-block-PTMO copolymer.

One of the main problems encountered during dispersion of carbon nanoparticles, like CNTs, GNPs, nCB limiting their effective use in polymer matrices, are the strong interfacial attraction between one another (CNTs-CNTs, GNPs-GNPs or nCB - nCB). Many approaches to overcome this issue have been made, however they mostly result in an excessive modification or even damage to the unique morphology of nanofiller. An efficient alternative allowing to tailor the polymer/nanofiller interface is mixing them together with a different shaped nanofiller (i.e. plate-like shape or powder-like). In the discussed study, it was assumed that application of graphene nanoplatelets might be a suitable solution. A uniform distribution of CNTs along with GNPs and/or nCBs should cause a synergistic effect and thus enable them to act together as stronger reinforcing agents for the polymer, resulting in a substantial enhancement of thermal and mechanical properties. All three types of nanoparticles were found to be well dispersed in the polymer matrix (Fig. 3), however in the case of PETG-*block*-PTMO/0.3nCB nanocomposites carbon black was almost not visible in SEM micrographs, since perhaps it was covered with polymer matrix. Both the SWCNTs and GNPs show fairly good distribution in Fig. 3 c and d. Additionally, the SEM image of PETG-*block*-PTMO/SWCNT+GNP in Fig.3 (c and d) show that the SWCNTs and graphene nanoplatelets form some kind of network structure. The SWCNTs appear to have a better affinity for GNPs than for nCB. This kind of conductive network formation due to graphene nanosheets may explain the good electrical conductivity results from PETG-*block*-PTMO/0.1SWCNT+0.1GNP+0.1nCB.

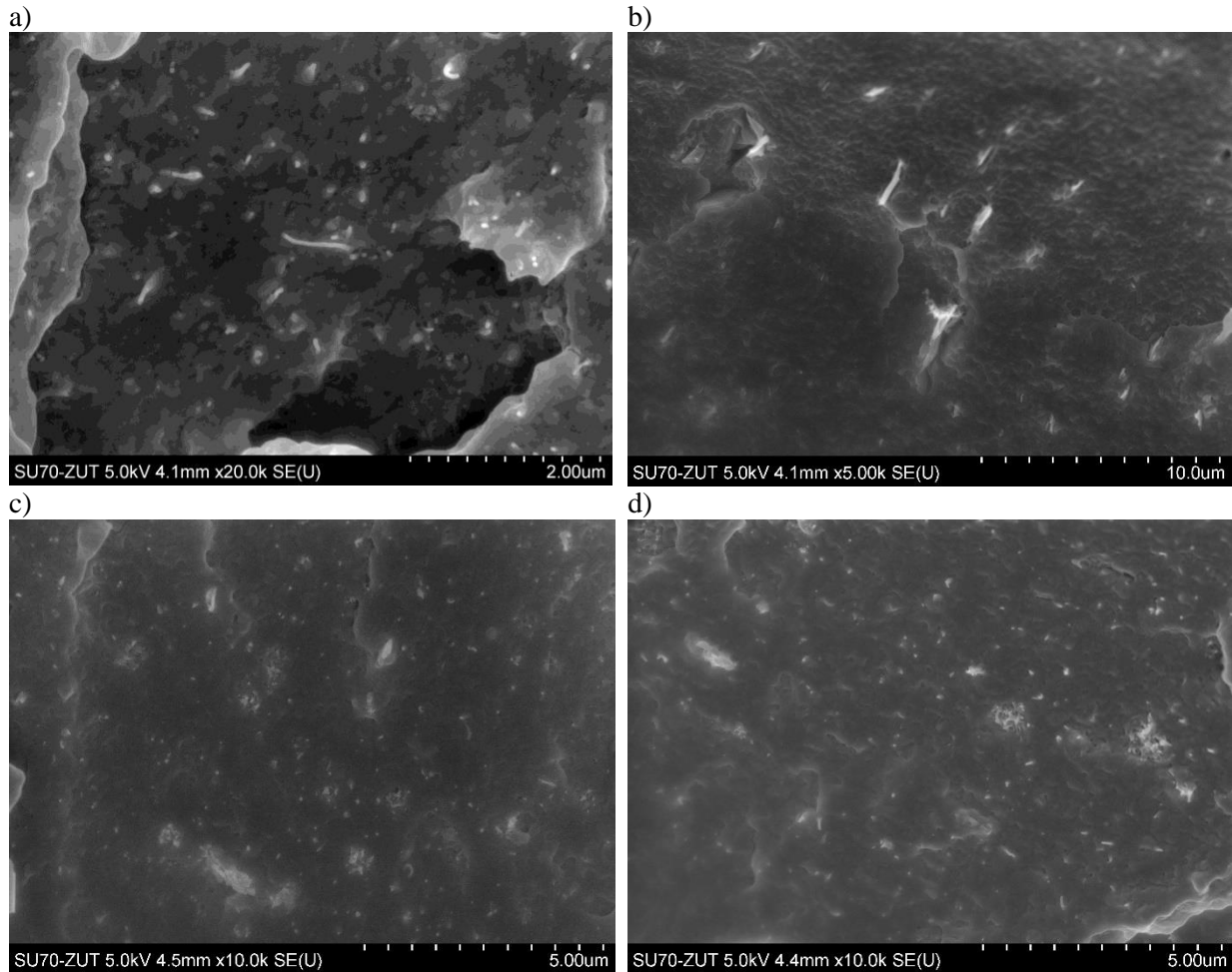


Figure 3: SEM micrographs of the series of nanocomposites based on: a) 0.3wt% of SWCNT, b) 0.3wt% of GNP, c) 0.15SWCNT+0.15GNP and d) 0.1SWCNT+0.1GNP+0.1nCB

In order to compare the influence of three types of nanofillers on the physicochemical properties of PETG-*block*-PTMO based nanocomposites, the i.e. number average molecular mass, intrinsic viscosity, melt flow index and density, were determined. The post-consumer foil PETG exhibits the number average molecular weight ( $M_n$ ) of 29 200 g/mol. In turn, the values of  $M_n$  for the series of nanocomposites based on PETG-*block*-PTMO ranged from 28 200 to 32 100 g/mol. The measured values of intrinsic viscosity for PETG-*block*-PTMO copolymer (0.72 dl/g) and PETG-*block*-PTMO hybrid nanocomposites (ca. 0.68) dl/g for three hybrids suggest that molecular masses of the all polymers are reasonable high. The presented in Table 1 values of intrinsic viscosity, melt viscosity and density are dependent on the sample composition. The value of  $[\eta]$  slightly decreased with addition of nanofillers, but with the increasing content of graphene platelets, this value increased. Additionally, nanofiller caused a decrease of MFI values, if compared to neat PETG-*block*-PTMO, that can result from the increase of the melt viscosity due to the polymer–nanofiller interactions. However, no effect on the glass transition temperature along with an addition of carbon nanofillers into the polymer matrix.

Sample	$Mn \cdot 10^4$ [g/mol]	$[\eta]$ [dl/g]	$d$ [g/cm <sup>3</sup> ]	MFI [g/10min]	$T_g$ [°C]
PETG	2.92	0.57	1.2356	4.12	69
PETG-PTMO	3.01	0.72	1.3567	3.95	-23
PETG-PTMO/0.3SWCNT	2.82	0.70	1.3462	2.65	-24
PETG-PTMO/0.3GNP	2.95	0.73	1.3581	3.90	-23
PETG-PTMO/0.3nCB	3.22	0.68	1.3725	2.95	-22
PETG-PTMO/0.15SWCNT+0.15GNP	3.05	0.68	1.3724	2.90	-24
PETG-PTMO/0.15SWCNT+0.15nCB	3.11	0.66	1.3921	2.85	-24
PETG-PTMO/0.1SWCNT+0.1GNP+0.1nCB	3.21	0.68	1.4103	2.17	-24

*Mn* – number average molar mass; *[\eta]* – intrinsic viscosity; *d* – density measured at 23°C; *MFI*- melt flow index; *T<sub>g</sub>* – glass transition temperature;

Table 1: Physico-chemical and gas barrier properties for the obtained nanocomposites based on PETG

Fig. 4 shows the alternating current conductivity,  $\sigma(F)$  as a function of frequency (F) for PETG-PTMO/SWCNT+GNP+nCB hybrid nanocomposites. Unfortunately at the concentration of 0.3 wt % both GNP and CB didn't cause any effect on the formation of electrical pathways in the PETG-*block*-PTMO based nanocomposites. The same observations were made for the hybrid PETG-*block*-PTMO/0.15GNP+0.15nCB. In turn, conducting networks have already been formed by 0.3 wt % SWCNT alone. However at the concentration of 0.15 wt % of SWCNT and 0.15 wt% of GNPs multiple electron pathways were provided through a synergy between the SWCNT and GNPs. Unfortunately, the addition of the same amount of nCB (0.15wt%) into 0.15wt% of SWCNT didn't cause any effect on the electrical conductivity of PETG-*block*-PTMO hybrid nanocomposite. The hybrid PETG-*block*-PTMO/0.15SWCNT+0.15GNP exhibited the behavior typical for semiconducting samples with the conductivity of  $10^{-6}$  S/cm. Probable explanation of enhancing the electrical conductivity of PTT-PTMO/SWCNT by GNP, which proved to be non-conductive, was that carbon nanotubes were hitched to the residual functionalized groups on the surface of graphene. Since these groups were "deactivated" by carbon nanotubes, the free movement of electrical charge was observed in case of PTT-PTMO hybrid nanocomposites

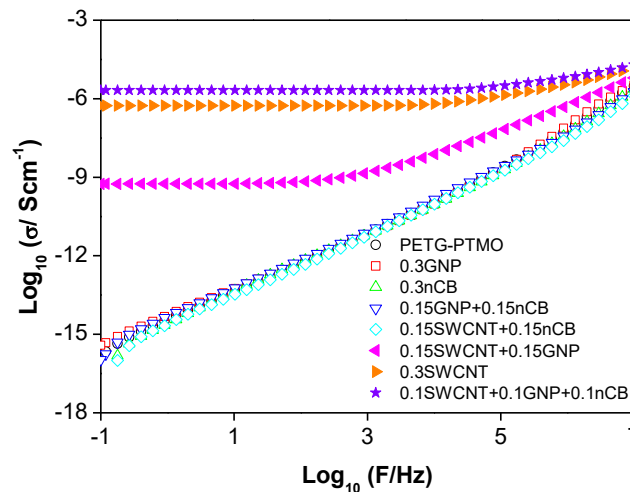


Figure 4: Alternating current conductivity,  $\sigma(F)$  as a function of frequency (F) for PETG-*block*-PTMO based nanocomposites.

The tensile properties of the PETG-*block*-PTMO/SWCNT+GNP+nCB hybrid nanocomposites were examined. As summarized in Table 2, there was a clear tendency that the stress at strain of 100% increases and elongation decreases with an increase of the total content of nanofillers. Carbon nanofillers (SWCNT, GNP, nCB) added in small amount to PETG-*block*-PTMO copolymer increases tension related to deformation, limiting the free length of chains which are located between physical nodes of the network / matrix (they create additional physical nodes). However, this effect was much stronger when at least two nanofillers were used. For pristine PETG-*block*-PTMO copolymer the stress at strain of 100% was 12.8 MPa. With the incorporation up to 0.3 wt % of SWCNT, this value increased to ca. 14.1 MPa, which is ca. 10 % lower than that of the neat block copolymer. GNP and nCB caused smaller increase of  $\sigma(100\%)$  of about 7-8%. The increase in the stress at strain of 100% was accompanied with decrease in the elongation at break for all synthesized nanocomposites. Thus the tensile measurements revealed that the effect of hybrid nanofillers system is more pronounced on the yield stress. The pronounced increase in the  $\sigma_y$  reflects the reinforcement effect was attained by the dispersion of the SWCNT/GNP and nCB in polymer matrix. Calorimetric studies for PETG-*block*-PTMO/hybrid nanocomposites proved that no melting/crystallization peaks were noticed. Therefore, the observed improvement in the tensile properties at low nanofillers' loading cannot be due to a change in crystallinity and is more likely caused by the presence of nanofillers. Similar results has been also previously observed for PTT-*block*-PTMO nanocomposites with montmorillonite (MMT) [19], graphene oxide (GO) [20] and hybrid system of SWCNT/GNP [21]. The synergistic toughening mechanisms of combination of SWCNT, GNP and nCB has been observed for PETG-*block*-PTMO copolymer.

Sample	$\sigma(100\%)$ MPa	$\sigma_y$ MPa	$\epsilon_y$ %	$\sigma_b$ MPa	$\epsilon_b$ %
PETG-PTMO	12.8 ± 0.1	13.4 ± 0.2	45.4 ± 1.3	20.3 ± 0.1	594 ± 12
PETG-PTMO/0.3SWCNT	14.1 ± 0.1	13.7 ± 0.1	49.6 ± 0.1	19.8 ± 0.2	564 ± 14
PETG-PTMO/0.3GNP	13.6 ± 0.1	14.0 ± 0.1	49.8 ± 0.8	19.2 ± 0.3	591 ± 29
PETG-PTMO/0.3nCB	13.9 ± 0.1	14.4 ± 0.1	48.1 ± 1.1	20.4 ± 0.2	512 ± 21
PETG-PTMO/0.15SWCNT+0.15GNP	14.1 ± 0.1	14.6 ± 0.9	47.6 ± 1.2	18.5 ± 1.2	542 ± 59
PETG-PTMO/0.15SWCNT+0.15nCB	13.6 ± 0.3	14.8 ± 0.2	47.8 ± 0.8	20.7 ± 0.6	517 ± 24
PETG-PTMO/0.1SWCNT+0.1GNP+0.1nCB	14.7 ± 0.1	15.1 ± 0.1	51.7 ± 0.5	19.9 ± 0.2	539 ± 13

$\sigma(100\%)$  – stress at strain of 100%;  $\sigma_y$ ,  $\epsilon_y$  – yield stress and strain respectively,  $\sigma_b$ ,  $\epsilon_b$  - stress and strain at break respectively

Table 2: Tensile properties of PETG-*block*-PTMO/SWCNT/GNP/nCB hybrid nanocomposites

#### 4 CONCLUSIONS

The potential of single-walled carbon nanotubes along with graphene nanoplatelets and carbon black as conductive nanofillers has been studied. SWCNT exhibited greater potential as functional nanofiller upon comparing with GNP and nCB due to their high purity and aspect ratio, resulting in the formation of conductive paths at lower content of nanoparticles. Dielectric spectroscopy along with mechanical properties enabled precise characterization of the morphological changes and to determine structure-electrical conductivity relationship. PETG-*block*-PTMO/GNP and PETG-*block*-PTMO/nCB nanocomposites found to be non-conductive at a content of 0.3 wt.%, which was perhaps due to large number of defects, free radicals and other irregularities on their surfaces. However, a significant synergistic effect between SWCNT, GNP and nCB on improving electrical conductivity and mechanical properties of nanocomposites based on modified post-consumer PETG foils has been observed. Heterogeneous structure of the PETG-*block*-PTMO allowed for a better and more uniform distribution of all types of nanoparticles and stabilized the structure in question. It is noteworthy to

underline the fact that in the case of hybrid system of 1D/2D/3D a positive hybrid effect has been observed. Moreover, by adjusting an optimum microstructure along with combination of 1D+2D+3D nanofillers' type it may lead to even higher improvement in electrical conductivity and mechanical properties and thus lowering the final price of the finished product.

### ACKNOWLEDGEMENTS

This work is the result of the research project GEKON2/O5/266860/24/2016 funded by the National Centre for Research and Development and National Fund for Environmental Protection and Water Management, Poland.

### REFERENCES

- [1] C. Kingston, R. Zepp, A. Andradý, A. Boverhof, R. Fehir, D. Hawkins, J. Roberts, P. Sayre, B. Shelton, Y. Sultan, V. Vejins, W. Wohlleben, Release characteristics of selected carbon nanotube polymer composites, *Carbon*, **68**, 2014, pp. 33-57 (doi: 10.1016/j.carbon.2013.11.042).
- [2] H. Kim, A.A. Abdala, C.W. Macosko, Graphene/Polymer Nanocomposites, *Macromolecules*, **43**, 2010, pp. 6515-6530 (doi: 10.1021/ma100572e).
- [3] J.C. Slonczewski, P.R. Weiss, Band Structure of Graphite, *Physical Review*, **109**, 1958, pp. 272 (doi: 10.1103/PhysRev.109.272)
- [4] C. Soldano, A. Mahmud, E. Dujardin, Production, properties and potential of grapheme, *Carbon*, **48**, 2010, pp. 2127-2150 (doi: 10.1016/j.carbon.2010.01.058).
- [5] K.S. Novoselov, A. K. Geim, S.V. Morozov, D. Jiang, Y. Shang, S.V. Dubonos, I.V. Grigorieva, A.A. Firsov, Electric Field Effect in Atomically Thin Carbon Films, *Science*, **306**, 2004, pp. 666-669 (doi: 10.1126/science.1102896).
- [6] C. Lee, X. Wei, J.W. Kysar, J. Hone, Measurement of the Elastic Properties and Intrinsic Strength of Monolayer Grapheme, *Science*, **321**, 2008, pp. 385-388 (doi: 10.1126/science.1157996).
- [7] A.A. Balandin, S. Ghosh, W. Bao, I. Calizo, D. Teweldebrhan, F. Miao, C.N. Lau, Superior Thermal Conductivity of Single-Layer Graphene, *Nano Letters*, **8**, 2008, pp. 902-907 (doi: 10.1021/nl0731872).
- [8] J.S. Bunch, S.S. Verbridge, J.S. Alden, A.M. van der Zande, J.M. Parpia, H.G. Graighead, P.L. McEuen, Impremeable Atomic Membranes from Grapheme Sheets, *Nano Letters*, **8**, 2008, pp. 2458-2462 (doi: 10.1021/nl801457b).
- [9] H. Kim, Y. Miura, C.W. Macosco, Graphene/Polyurethane Nanocomposites for Improved Gas Barrier and Electrical Conductivity, *Chemistry of Materials*, **22**, 2010, pp. 3441-3450 (doi: 10.1021/cm100477v).
- [10] M. El Achaby, F.A. Arrakhiz, S. Vaudreuil, A.K. Qaiss, M. Bousmina, O. Fassi-Fehri, Mechanical, Thermal, and Rheological Properties of Graphene-Based Polypropylene Nanocomposites Prepared by Melt Mixing, *Polymer Composites*, **33**, 2012, pp. 733-744 (doi: 10.1002/pc.22198).
- [11] J. Hwang, J. Muth, T. Ghosh, Electrical and Mechanical Properties of Carbon-Black-Filled, Electrocpun Nanocomposite Fiber Webs, *Journal of Applied Polymer Science*, **104**, 2007, pp. 2410-2417 (doi: 10.1002/app.25914).
- [12] S.Y. Yang, W.N. Lin, Y.L. Huang, H.W. Tien, J.Y. Wang, C.C.M. Ma, S.M. Li, Y.S. Wang, Synergetic effects of grapheme platelets and carbon nanotubes on the mechanical and thermal

- properties of epoxy composites, *Carbon*, **49**, 2011, pp. 793-803 (doi: 10.1016/j.carbon.2010.10.014).
- [13] A. Szymczyk, J. Nastalczyk, R.J. Sablong, Z. Roslaniec, The influence of soft segment length on structure and properties of poly(trimethylene terephthalate)-block-poly(tetramethylene oxide) segmentem random copolymers, *Polymers Advanced Technologies*, **22**, 2011, pp. 72-83 (doi: 10.1002/pat.1858).
- [14] F. Kremer, A. Schonhals, *Broadband Dielectric Spectroscopy*, Springer-Verlag, Heidelberg, 2003.
- [15] J. Hu, Y. Li, C. Li, W. Chen, D. Yang, Mechanical properties of fluorinated ethylene propylene (FEP) foils in use for neutrino detector project, *Polymer Testing*, **59**, 2017, pp. 362-370 (doi: 10.1016/j.polymertesting.2017.02.016).
- [16] N. Benipal, J. Qi, J.C. Gentile, W. Li, Direct glycerol fuel cell with polytetrafluoroethylene (PTFE) thin film separator, *Renewable Energy*, **105**, 2017, pp. 647-655 (doi: 10.1016/j.renene.2016.12.028).
- [17] T. Chen, W. Zhang, J. Zhang, Alkali resistance of poly(ethylene terephthalate) (PET) and poly(ethylene glycol-co-1,4-cyclohexanedimethanol terephthalate) (PETG) copolyesters: The role of composition, *Polymer Degradation and Stability*, **120**, 2015, pp. 232-243 (doi: 10.1016/j.polymdegradstab.2015.07.008).
- [18] T. Chen, G. Jiang, G. Li, Z. Wu, J. Zhang, Poly(ethylene glycol-co-1,4-cyclohexanedimethanol terephthalate) random copolymers: effect of copolymer composition and microstructure on the thermal properties and crystallization behaviour, *RSC Advances*, **5**, 2015, pp. 60570-60580 (doi: 10.1039/C5RA09252C).
- [19] A. Szymczyk, S. Paszkiewicz, Z. Roslaniec, Influence of intercalated organoclay on the phase structure and physical properties of PTT-PTMO block copolymers, *Polymer Bulletin*, **70**, 2012, pp. 1575-90 (doi: 10.1007/s00289-012-0859-y).
- [20] S. Paszkiewicz, A. Szymczyk, Z. Spitalsky, J. Mosnacek, K. Kwiatkowski and Z. Roslaniec, Structure and properties of nanocomposites based on PTT-block-PTMO copolymer and graphene oxide by in situ polymerization, *European Polymer Journal, Macromolecular Nanotechnology*, **50**, 2014, pp. 69-77 (doi: 10.1016/j.eurpolymj.2013.10.031).
- [21] S. Paszkiewicz, A. Szymczyk, X.M. Sui, H.D. Wagner, A. Linares, T.A. Ezquerria and Z. Roslaniec, Synergetic effect of single-walled carbon nanotubes (SWCNT) and graphene nanoplatelets (GNP) in electrically conductive PTT-block-PTMO hybrid nanocomposites prepared by in situ polymerization, *Composites Science and Technology*, **118**, 2015, pp. 72-77 (doi: 10.1016/j.compscitech.2015.08.011).